SCIENCE CHINA
Physics, Mechanics & Astronomy

• Article •

July 2014 Vol. 57 No. 7: 1283–1288
doi: 10.1007/s11433-014-5480-7

Mode splitting of a cavity with a high-density birefringence rubidium vapor in the superstrong coupling regime†

CHEN LiangChao, YU XuDong, MENG ZengMing & ZHANG Jing*

State Key Laboratory of Quantum Optics and Quantum Optics Devices, Institute of Opto-Electronics, Shanxi University, Taiyuan 030006, China

Received March 8, 2014; accepted April 14, 2014; published online April 30, 2014

The mode splitting in a system with Doppler-broadened high-density two-level atoms in the presence of magnetic field inside a relatively long optical cavity is studied in the superstrong coupling regime (atoms-cavity coupling strength $g\sqrt{N}$ is near or larger than the cavity free-spectral range Δ_{FSR}). The effect of a magnetic field applied along the quantization axis is used to break the polarization degeneracy of the cavity and thereby introduce birefringence (or Faraday rotation) into the medium. The cavity modes are further split in the presence of the magnetic field compared with the normal case of the multi-normal-mode splitting of the two-level system near the D2 line of ^{87}Rb. The dependence of the mode splitting on the magnetic field and the temperature is studied. The theoretical analysis according to the linear dispersion theory can provide a good explanation.

superstrong coupling, normal-mode splitting, Zeeman effect, birefringence

PACS number(s): 32.60.+i, 33.55.+b, 42.50.Ct

Citation: Chen L C, Yu X D, Meng Z M, et al. Mode splitting of a cavity with a high-density birefringence rubidium vapor in the superstrong coupling regime. Sci China-Phys Mech Astron, 2014, 57: 1283–1288, doi: 10.1007/s11433-014-5480-7

1 Introduction

The multi-atom and cavity system has attracted much attention in the cavity-quantum electrodynamics (C-QED) because the atomic ensemble can remarkably enhance the coherent radiation and the coupling strength. The strong coupling is vital in C-QED, which is characterized by $g > \kappa, \gamma$ (g is the single-photon coupling strength, κ is the cavity decay rate, and γ is the atomic decay rate) in the single atom and cavity system [1–4]. For the multi-atom system, the coupling strength is increased to $g\sqrt{N}$ (N is the atom number) [5,6]. Compared with the single atom–cavity system in which one needs to operate the single atoms and decrease the cavity volume and make the cavity with high finesse simultaneously, it is relatively easy to realize the strong coupling condition for the multi-atom and cavity system even with a low-finesse cavity because the atom number can be increased by raising the temperature in the hot atom vapor medium [7,8]. Recently, a new regime, that is, the superstrong coupling condition (the coupling strength is near or larger than the free spectrum range of the cavity), has been theoretically discussed [9,10], in which some interesting phenomena and new applications are expected. The superstrong coupling condition is experimentally demonstrated in the Doppler-broadened degenerate two-level atoms and cavity system by coupling many atoms into the cavity mode [11]. In the experiment, more than one longitudinal mode (0 mode) "see" and interact with the atoms. Hence, the normal-mode splitting can occur for the adjacent cavity modes.

In this paper, we present the study of the two-level atoms and cavity system in the superstrong coupling regime in the presence of magnetic field. When the inhomogeneously broadened two-level atoms are in a long optical cavity, the

*Corresponding author (email: jzhang74@sxu.edu.cn)
†Contributed by ZHANG Jing (Associate Editor)

atomic density can be easily increased by the temperature to satisfy this superstrong coupling condition. We apply a magnetic field which is parallel to the axis of the cavity. Hence, the Zeeman sublevels are shifted and split. The right and left circularly polarized components of the cavity mode interact with the nondegenerate Zeeman transitions. This induces the birefringence and splits the degenerate normal modes. The multi-normal-mode splitting in the birefringence medium is observed in the superstrong coupling regime. We find that the separation of the splitting is increased when the magnetic field or the temperature rises. The splitting of the nondegenerate two-level atoms and cavity system can be well explained by the linear dispersion theory. The birefringence-induced and cavity-enhanced multi-normal-mode splitting can be potentially used to generate the multi-mode entangled states and to construct high-sensitivity magnetometer [12–15].

2 Theoretical analysis

The Zeeman energy-levels degenerate two-level atoms interact with the monochromatic plane light field, and the master equations of the system can be expressed as:

$$\dot{\rho}_{ij} = -\left(\mathrm{i}\omega_{ij} + \frac{\gamma}{2}\right)\rho_{ij} - \frac{\mathrm{i}}{\hbar}\boldsymbol{E}_{\mathrm{c}}\exp(-\mathrm{i}\omega t)\boldsymbol{\mu}_{ij}w, \tag{1}$$

$$\dot{w} = -\gamma(w+1) + \frac{2\mathrm{i}}{\hbar}[\boldsymbol{E}_{\mathrm{c}}\exp(-\mathrm{i}\omega t)\boldsymbol{\mu}_{ij}\rho_{ji} - \rho_{ij}\boldsymbol{E}_{\mathrm{c}}^{*}\exp(\mathrm{i}\omega t)\boldsymbol{\mu}_{ji}], \tag{2}$$

where $\rho_{ij,ji}$ is the matrix element of density operator, i, j denote the excited and ground states, respectively, ω_{ij} is the transition frequency between i,j, and ω is the frequency of light. $w = \rho_{ii} - \rho_{jj}$ is called population inversion. $\boldsymbol{\mu}_{ij} = \langle i|(-e\hat{\boldsymbol{r}})|j\rangle$ is the electric dipole moment. γ is the decay rate of the excited state. $\boldsymbol{E}_{\mathrm{c}}$ is the amplitude of the electric field component of the light. Applying the slow-varying approximation, we can obtain the steady-state solution of eqs. (1) and (2):

$$\tilde{\rho}_{ij} = \frac{\boldsymbol{E}_{\mathrm{c}}\boldsymbol{\mu}_{ij}w}{\hbar(\Delta + \mathrm{i}\gamma/2)}, \tag{3}$$

$$w = -\frac{1 + 4\Delta^2/\gamma^2}{1 + 4\Delta^2/\gamma^2 + 8\Omega^2/\gamma^2}, \tag{4}$$

where $\tilde{\rho}_{ij} = \rho_{ij}\exp(\mathrm{i}\omega t)$ is the slowly varying quantity, $\Delta = \omega - \omega_{ij}$, and $\Omega = |\boldsymbol{\mu}_{ij}\boldsymbol{E}_{\mathrm{c}}|/\hbar$. Since $\boldsymbol{P}(t) = \boldsymbol{P}\exp(-\mathrm{i}\omega t) + c.c. = N_{\mathrm{D}}(\boldsymbol{\mu}_{ji}\rho_{ij} + \boldsymbol{\mu}_{ij}\rho_{ji})$ and $\boldsymbol{P} = \varepsilon_0\chi\boldsymbol{E}_{\mathrm{c}}$, where N_{D} is the atomic number density, the susceptibility can be written as:

$$\chi = \frac{2N_{\mathrm{D}}|\boldsymbol{\mu}_{ij}|^2}{\varepsilon_0\hbar\gamma}\frac{\mathrm{i} - 2\Delta/\gamma}{1 + 4\Delta^2/\gamma^2 + 8\Omega^2/\gamma^2}. \tag{5}$$

If the atoms are placed in the magnetic field, the Zeeman sublevels are shifted by an amount δ, which is approximately proportional to the strength of magnetic field when the magnetic field is in the weak-field regime, and the second-order Zeeman effect appears when the magnetic field is strong [16,17]. Hence, the detuning of the laser and the atomic transition becomes $\Delta' = \Delta - \delta$ and the atom-cavity detuning is $\Delta'_{\mathrm{ac}} = \Delta_{\mathrm{ac}} - \delta$. According to the linear dispersion theory, the intensity-absorption coefficient and the refractive index of the atomic medium are $\alpha = 2\omega\mathrm{Im}[\chi]/c$ and $n = 1 + \mathrm{Re}[\chi]/2$ if $|\chi| \ll 1$, and then the intensity-absorption coefficient and the refractive index can be written as:

$$n = 1 - \frac{2N_{\mathrm{D}}|\boldsymbol{\mu}_{ij}|^2}{\varepsilon_0\hbar}\frac{\Delta - \delta}{\gamma^2 + 4(\Delta - \delta)^2 + 8\Omega^2}, \tag{6}$$

$$\alpha = \frac{2N_{\mathrm{D}}\omega|\boldsymbol{\mu}_{ij}|^2}{\varepsilon_0\hbar c}\frac{\gamma}{\gamma^2 + 4(\Delta - \delta)^2 + 8\Omega^2}. \tag{7}$$

Also, when the large detuning condition ($\Delta - \delta >> \Omega,\ \gamma$) is satisfied, eqs. (6) and (7) can be simplified as:

$$n = 1 - \frac{N_{\mathrm{D}}|\boldsymbol{\mu}_{ij}|^2}{\varepsilon_0\hbar}\frac{1}{2(\Delta - \delta)}, \tag{8}$$

$$\alpha = \frac{N_{\mathrm{D}}\omega|\boldsymbol{\mu}_{ij}|^2}{\varepsilon_0\hbar c}\frac{\gamma}{2(\Delta - \delta)^2}. \tag{9}$$

According to the selection rule, the left circularly polarized and right circularly polarized components of the intracavity field drive the transitions with $\Delta m = \pm 1$, respectively, where m is the projection of angular momentum along the quantization axis. If σ^+ transition is shifted by $\delta^+ = \delta$, then σ^- transition is shifted by $\delta^- = -\delta$ correspondingly [18,19]. So, the left circularly polarized light and right circularly polarized light will correspond to different optical susceptibilities. Those results are consistent with ref. [20], in which the properties of large dispersion and less absorption in a large detuning regime are used to change the polarization of a linearly polarized light with high fidelity and low absorption.

Now we consider the transmission of the atomic vapor medium and a standing wave cavity system. The lengths of the medium and the cavity are l and L, respectively. So, the free spectrum range for the vacuum cavity is $\Delta_{\mathrm{FSR}} = \pi c/L$. The intensity transmissivity (reflectivity) of the input and output mirrors of the cavity are T_1, T_2 (R_1, R_2), respectively. Hence, the finesse is $F = \pi(R_1R_2)^{1/4}/(1 - \sqrt{R_1R_2})$ and the linewidth is $\kappa = \Delta_{\mathrm{FSR}}/F$. The transmission of the coupled atom–cavity system can be expressed as [10,21]:

$$T(\Delta) = \frac{T^2A_{\mathrm{int}}\mathrm{e}^{-\alpha l}}{(1 - RA_{\mathrm{int}}\mathrm{e}^{-\alpha l})^2 + 4RA_{\mathrm{int}}\mathrm{e}^{-\alpha l}\sin^2(\Phi/2)}, \tag{10}$$

where $T = \sqrt{T_1T_2}$ and $R = \sqrt{R_1R_2}$, A_{int} is the intracavity loss, $\Phi(\Delta) = 2\pi(\Delta - \Delta_{\mathrm{ac}})/\Delta_{\mathrm{FSR}} + 2(n-1)\omega l/c$ is the round-trip phase shift function of the laser, Δ is the detuning of the laser and the atomic transition, and Δ_{ac} is the atom-cavity detuning. Here, it should be noticed that the left (right) circularly polarized light is defined according to the propagating direction of light. The left (right) circularly polarized light inside the cavity will be transformed into right (left) circularly polarized light once reflected by the cavity mirror, but since the relative

direction between the light and magnetic field (the quantization axis) is also changed simultaneously, the resulting right (left) circularly polarized light will drive the same transition as transformed before. So, the transmission function for the left (right) circularly polarized light can be obtained by the usual method of multibeam interference.

Figure 1 is the theoretical calculation of the transmission spectra of the two-level atomic medium-cavity system. Parameters used in plotting Figure 1 have been tried to simulate the ones in our experiment. The vertical scale is normalized to the transmission of the cavity. In Figure 1(a), the coupling strength $g\sqrt{N}$ is larger than κ, γ, but smaller than the free spectrum range. So the 0 mode, which is resonant with the degenerate two-level transition frequency, is split into two peaks because the phase shift function has two real solutions except for $\Delta = 0$ GHz. In Figure 1(b), the coupling strength is larger than the free spectrum range, which satisfies the super-strong coupling condition, the adjacent modes ($k = \pm 1, \pm 2$) can also interact with the atoms, and are divided into two peaks, and the split normal modes are located at the two sides of the two-level transition frequency. The heights of two peaks are asymmetric because of the detuning of the intracavity modes. Figure 1(c) corresponds to Figure 1(a) when we apply a magnetic field which shifts the Zeeman sublevels by $\delta^+ = -\delta^- = 2\pi\times 56$ MHz, the normal modes, including the split 0 modes, are further split because Zeeman shift changes the detuning of the atom and the intracavity fields (the right and left circularly polarized components of the cavity mode). Figure 1(d) corresponds to Figure 1(b); the degenerate normal modes ($k = \pm 1, \pm 2$) are broken when the magnetic field is applied. The separations of the nondegenerate peaks depend on the strength of the magnetic field, the atomic number density, and the detuning of the intracavity field and the atomic transition according to eq. (6). For Doppler-broadened hot atoms, it is approximately valid to replace γ by the Doppler width $\delta\omega_{\rm D} = \omega\sqrt{2k_{\rm B}T/m}/c$ ($\delta\omega_{\rm D} = 2\pi\times 351$ MHz in 120 °C, as a comparison, $\gamma = 2\pi\times 6.07$ MHz for cold rubidium atoms) to include the Doppler-broadening effect [11]. When drawing Figure 1, we find that choosing $\gamma = 0.08\times\delta\omega_{\rm D}$ gives a better fit with the experimental result. Since the large detuning condition $\Delta - \delta \gg \Omega, \gamma$ is not satisfied anymore, we just take the separations as:

$$\Delta_{\rm gap} = \omega\frac{l}{L}\frac{N_{\rm D}|\boldsymbol{\mu}|^2}{\varepsilon_0\hbar}\frac{\delta}{\gamma^2/4 + (\Delta-\delta)^2 + 2\Omega^2}. \tag{11}$$

So, increasing the atomic number density $N_{\rm D}$ can enlarge the normal-mode splitting. For a certain mode, increasing the strength of the magnetic field can increase the splitting of the degenerate normal mode. The separation of the split degenerate normal modes close to the atomic transition is larger than the ones far away from the atomic transition since the small detuning makes $\delta/[\gamma^2/4 + (\Delta-\delta)^2 + 2\Omega^2]$ large.

3 Experimental result

The experiment setup is shown in Figure 2. A DBR diode

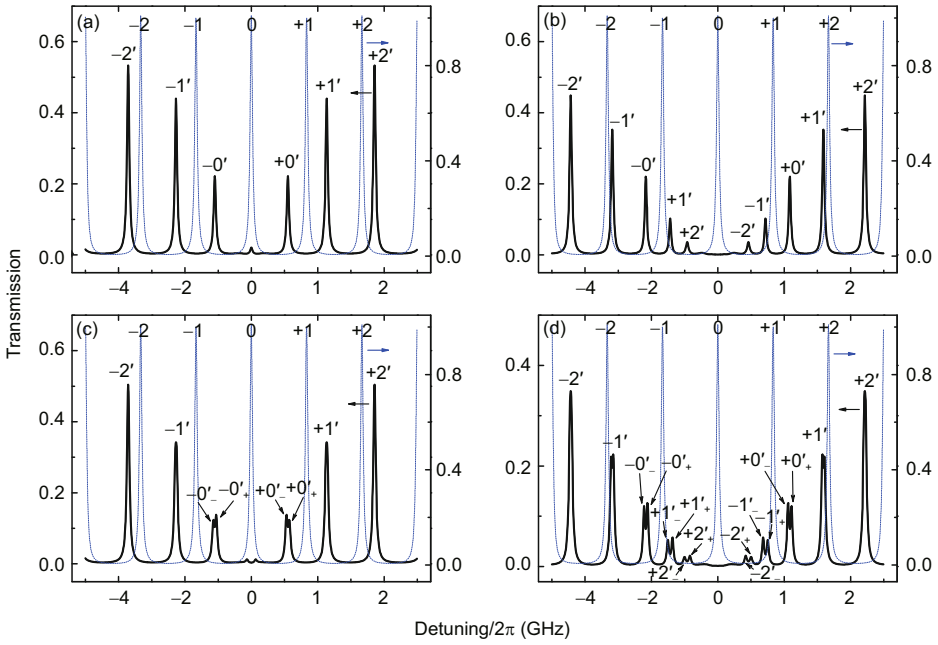

Figure 1 (Color online) Theoretical calculation of the transmission spectra of the two-level atoms and cavity system. The dotted blue lines in (a)–(d) are the transmission spectra of the vacuum cavity. The free spectrum range of the cavity is $\Delta_{\rm FSR} = 2\pi\times 833$ MHz, the finesse is 54, the wavelength of the laser is 780 nm, and length of the atomic medium is 5 cm. $k = \pm 0', \pm 1', \pm 2'$ correspond to the normal-mode splitting peaks of the degenerate two-level atoms and cavity system ($\Phi = k\times 2\pi$). $k = \pm 0'_{\pm}, \pm 1'_{\pm}, \pm 2'_{\pm}$ label the normal-mode splitting peaks of the nondegenerate two-level atoms and cavity system for the right and left circularly polarized components of the cavity field. The other parameters: (a) $N_{\rm D} = 1.6\times 10^{17}$ m^{-3} and $\delta^+ = -\delta^- = 0$ MHz; (b) $N_{\rm D} = 5.4\times 10^{17}$ m^{-3} and $\delta^+ = -\delta^- = 0$ MHz; (c) $N_{\rm D} = 1.6\times 10^{17}$ m^{-3} and $\delta^+ = -\delta^- = 2\pi\times 56$ MHz and (d) $N_{\rm D} = 5.4\times 10^{17}$ m^{-3} and $\delta^+ = -\delta^- = 2\pi\times 56$ MHz.

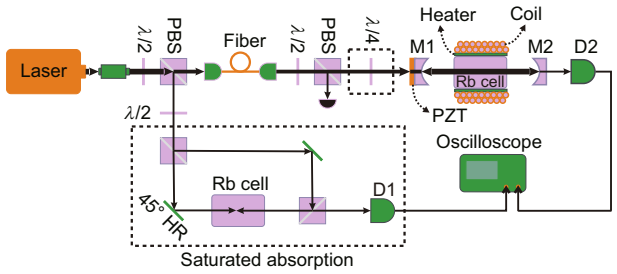

Figure 2 (Color online) Schematic drawing of the experimental setup. $\lambda/2$: half-wave plate; $\lambda/4$: quarter-wave plate; PBS: polarized beam splitter; D1-2: detector; M1-2: concave mirror of the cavity and PZT: piezoelectric transducer, which is used to adjust the length of the cavity. The copper coil is used to produce the magnetic field. The temperature of Rb cell is controlled by a heater.

laser is used with a frequency scanning in the vicinity of ^{87}Rb D2 line ($F = 1 \rightarrow F' = 0, 1, 2$). The $\lambda/2$ wave plate and polarized beam splitter (PBS) are used to separate the laser into two parts. One is injected into the cavity, and the other is used for frequency reference. The frequency reference is obtained by the saturated absorption spectrum, in which pump and probe beams counterpropagate with each other in the naturally mixed rubidium cell. The signal of saturated absorption is monitored by detector D1. The other laser passes through a single-mode polarization-maintaining optical fiber. The $\lambda/2$ wave plate and PBS after the fiber are used to control the intensity of the incident light of cavity. In our experiment, the power of the incident beam is about 3.0 mW. The cavity is composed of two concave mirrors (M1 and M2), whose radiuses of curvature are both 10 cm. The reflectivity of M1 is $R_1 = 90\%$, and the one of M2 is $R_2 = 99.9\%$. The length of the cavity is 18 cm, and a naturally mixed Rb atom vapor cell with a length of 5 cm is put at the center of the cavity. A pair of coils provide a bias magnetic field for the atoms. The temperature of the atomic cell is controlled by a heater. If a magnetic field is applied, the quantization axis is usually to be in the direction of the magnetic field for the convenience of calculation of Hamiltonian of the atoms interacting with the light. Since the magnetic field in our experiment is parallel to the direction of the light, it's reasonable to decompose the light into left circularly polarized component and right circularly polarized component. Percentage of the two components can be changed continuously from 0% to 100% by rotating the $\lambda/4$ wave plate.

In the experiment, we first study the degenerate two-level atoms and cavity system (the magnetic field $B = 0$ G), as shown in Figures 3(a) and (b). In Figure 3(a), the temperature of the Rb cell is 120 °C, the atom number is large enough and make the coupling strength $g\sqrt{N}$ larger than κ and γ. When the strong coupling condition is satisfied, the resonant mode (0 mode) is split into two peaks. The peaks at the blue detuning side are obvious, but the others at the red detuning side can not be seen because of the squash effect of another transition (^{85}Rb D2 line $F = 2 \rightarrow F' = 1, 2, 3$). So, we do not plot this part in Figure 3. In Figure 3(b), the temperature is further increased to 160 °C and the coupling strength is larger than the free spectrum range; the more adjacent modes begin to be split into two asymmetric peaks. Then, we apply a magnetic field with $B = 84$ G (correspondingly, δ is about $2\pi \times 56$ MHz), as shown in Figures 3(c) and (d). Figures 3(c) and (d)

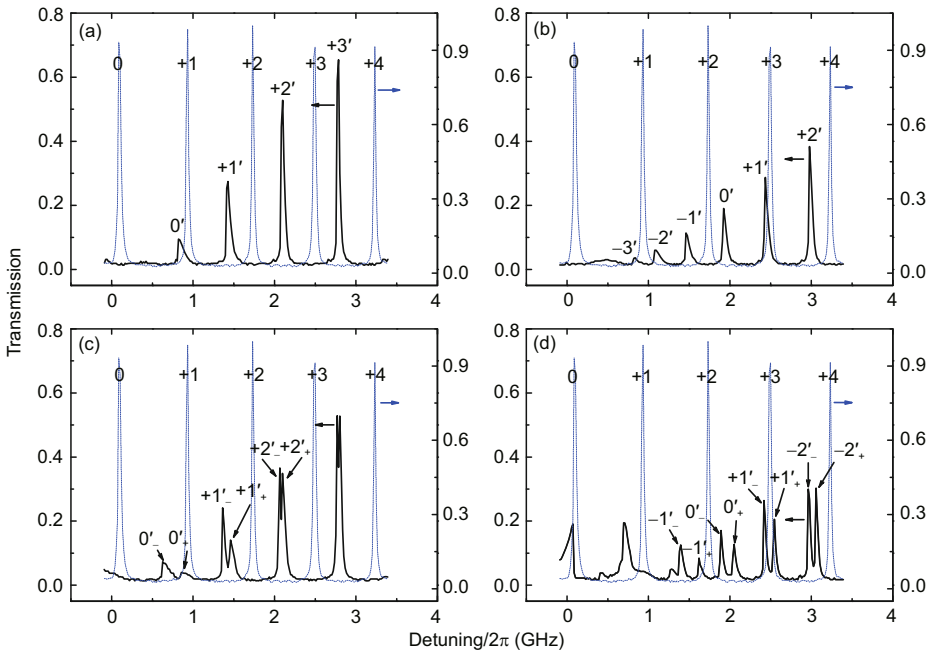

Figure 3 (Color online) The measurement of the cavity transmission by scanning the frequency of the laser. The power of the input light is about 3.0 mW. The blue dashed lines in the four figures are the transmission of the empty cavity, which is used as a reference. The black lines are the transmission of the atom-cavity system. In (a) and (c), the temperature is 120 °C, in (b) and (d), the temperature is increased to 160 °C. Parts (a) and (b) are the results with no magnetic field applied, and (c) and (d) respond to the magnetic field of 84 G. The transmissions have been normalized to the reference line.

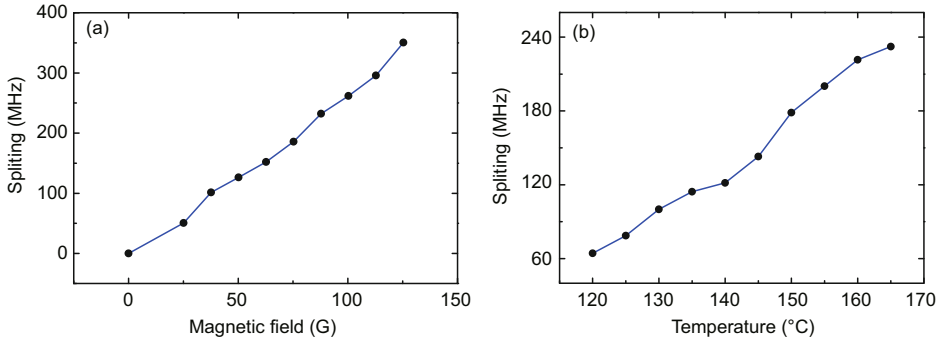

Figure 4 (Color online) The dependence of the mode splitting on the magnetic field (a) and temperature (b). In (a), the temperature is fixed at 165 °C. The power of the incident light is 3.0 mW. The mode we measured is the $k = -1'$ mode with a detuning to the two-level atoms of $2\pi \times 1.85$ GHz. In (b), the magnetic field is 84 G. The detuning to the two-level atoms is $2\pi \times 2.47$ GHz. The incident light has a power of 3.0 mW. The temperatures are increased from 120 °C to 165 °C in steps of 5 °C.

correspond to Figures 3(a) and (b) with the same other parameters. The right and left circularly polarized components of the cavity modes interact with different Zeeman transitions. The normal modes for the degenerate two-level atoms and cavity system are further split into two peaks corresponding to the right and left circularly polarized lights because the Zeeman shift has changed the detunings of the light-atom and atom-cavity. In Figure 3 (c), the $0'$ mode and the other modes ($k = +1', +2', +3'$) are split under the strong coupling condition. In Figure 3(d), the new modes $k = -3', -2', -1'$ and the other modes ($k = 0', +1', +2'$) are divided under superstrong coupling strength condition. We can see in Figure 3(d) that the split components of modes $k = -3', -2'$ merge into a larger peak.

Figure 4 shows the dependence of the splitting width of the mode ($k = -1'$) on the magnetic field and the temperature. The splitting of the $-4'$ mode is largest, but its peaks are very small due to the larger loss, so we choose the $-1'$ mode in Figure 4. According to eq. (11), it is obvious that the splitting width is proportional to the Zeeman shift. In Figure 4(a), the slope of the splitting via the magnetic field is 2.6 MHz/G, which indicates that the splitting width is very sensitive to the magnetic field. Thus, this opens a new way to measure the magnetic field with high sensitivity and high resolution. The resolution of our system is limited by the linewidth of the cavity. However, some studies on high-finesse cavity have been reported [22]. Figure 4(b) shows the splitting of the degenerate mode having a detuning to the atomic transition of $2\pi \times 2.47$ GHz with the temperature increased from 120 °C to 165 °C in steps of 5 °C. The relation between the splitting width and the temperature is caused by the atomic number density in the Rb cell. With data from Figure 4(b) and eq. (11), we can calculate the number density of ^{87}Rb atoms in the cell at a specific temperature. It should be noticed that although it's very difficult to theoretically get an exact value of the number density of ^{87}Rb atoms in a specific container, an approximate calculation can be made based on the reference of rubidium 87 D line data (http://steck.us/alkalidata). Such calculation gives a value that is about one order of magnitude larger than the value calculated from our experimental result. We think that's mainly due to a large fraction of atoms populated at $5S_{1/2}, F = 2$ when without a pump light [8].

Finally, we study the polarization of the split nondegenerate modes of the cavity transmission by rotating the $\lambda/4$ wave plate before the cavity, as shown in Figure 5. According to the theoretical calculation, the left circularly polarized light causes the negative phase shift and the right circularly polarized light leads to the positive phase shift. Consequently the peaks corresponding to the left circularly polarized light appear at the relatively blue detuning side and the peaks

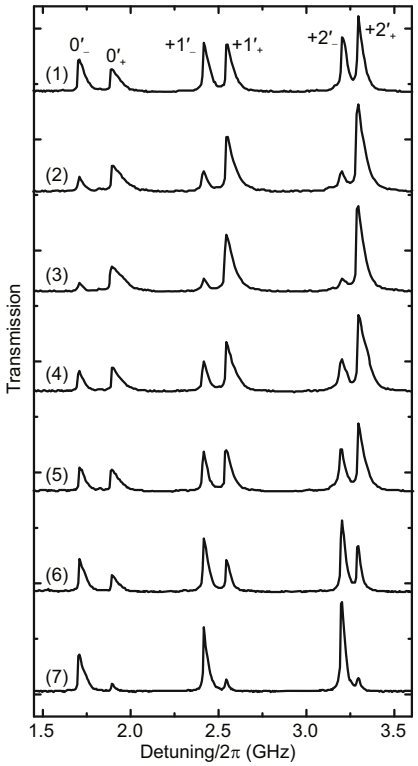

Figure 5 The transmission of the cavity by scanning the frequency of the laser and fixing the length of the cavity. The direction of the fast axis of $\lambda/4$ wave plate is changed. (1)–(7) correspond to the angles changing from 0 to $3\pi/4$ in steps of $\pi/8$. The temperature of the Rb vapor is 140 °C, and the magnetic field is $B = 84$ G.

corresponding to the right circularly polarized light appear at the relatively red detuning side of the original degenerate mode. Adjusting the angle of the polarization of the laser and the direction of the fast axis of the $\lambda/4$ wave plate can change the ratio of the right and left circularly polarized lights.

4 Conclusion

We have studied the nondegenerate two-level atomic medium-cavity system in the superstrong coupling regime. The normal modes are further split when we apply a magnetic field which shifts the Zeeman transitions. The separation is very sensitive to the intensity of the magnetic field. This work may be potentially used in the quantum information process and the measurement of the weak magnetic field.

This work was supported by the National Basic Research Program of China (Grant No. 2011CB921601), the National Natural Science Foundation of China (Grant No. 11234008), the NSFC Project for Excellent Research Team (Grant Nos. 61121064 and 11234008) and the Doctoral Program Foundation of the Ministry of Education China (Grant No. 20111401130001).

1 McKeever J, Boca A, Boozer A D, et al. Experimental realization of a one-atom laser in the regime of strong coupling. Nature, 2003, 425: 268–271
2 McKeever J, Boca A, Boozer A D, et al. Deterministic generation of single photons from one atom trapped in a cavity. Science, 2004, 303: 1992–1994
3 Aoki T, Dayan B, Wilcut E, et al. Observation of strong coupling between one atom and a monolithic microresonator. Nature, 2006, 443: 671–674
4 Thompson R J, Rempe G, Kimble H J. Observation of normal-mode splitting for an atom in an optical cavity. Phys Rev Lett, 1992, 68: 1132–1135
5 Tavis M, Cummings F W. Exact solution for an *N*-molecule-radiation-field hamiltonian. Phys Rev, 1968, 170: 379–384
6 Agarwal G S. Vacuum-field Rabi splittings in microwave absorption by Rydberg atoms in a cavity. Phys Rev Lett, 1984, 53: 1732–1734
7 Wang H, Goorskey D J, Burkett W H, et al. Cavity-linewidth narrowing by means of electromagnetically induced transparency. Opt Lett, 2000, 25: 1732–1734
8 Wu H B, Gea-Banacloche J, Xiao M. Observation of intracavity electromagnetically induced transparency and polariton resonances in a Doppler-broadened medium. Phys Rev Lett, 2008, 100: 173602
9 Meiser D, Meystre P. Superstrong coupling regime of cavity quantum electrodynamics. Phys Rev A, 2006, 74: 065801
10 Yu X D, Zhang J. Multi-normal mode-splitting for an optical cavity with electromagnetically induced transparency medium. Opt Express, 2010, 18: 4057–4065
11 Yu X D, Xiong D Z, Chen H X, et al. Multi-normal-mode splitting of a cavity in the presence of atoms: A step towards the superstrong-coupling regime. Phys Rev A, 2009, 79: 061803
12 Sycz K, Gawlik W, Zachorowski J. Resonant Faraday effect in a Fabry-Perot cavity. Opt Appl, 2010, 40(3): 633–639
13 Budker D, Gawlik W, Kimball D F, et al. Resonant nonlinear magneto-optical effects in atoms. Rev Mod Phys, 2002, 74: 1153–1201
14 Budker D, Kimball D F, Rochester S M, et al. Sensitive magnetometry based on nonlinear magneto-optical rotation. Phys Rev A, 2000, 62: 043403
15 Budker D, Yashchuk V, Zolotorev M. Nonlinear magneto-optic effects with ultranarrow widths. Phys Rev Lett, 1998, 81: 5788–5791
16 Roberts G J, Baird P E G, Brimicombe M W S M, et al. The Faraday effect and magnetic circular dichroism in atomic bismuth. J Phys B-At Mol Opt Phys, 1980, 13: 1389–1402
17 Chen X, Telegdi V L, Weis A. Magneto-optical rotation near the caesium D2 line (Macaluso-Corbino effect) in intermediate fields: I. Linear regime. J Phys B-At Mol Opt Phys, 1987, 20: 5653–5662
18 Maguire L P, Bijnen R M W V, Mese E, et al. Theoretical calculation of saturated absorption spectra for multi-level atoms. J Phys B-At Mol Opt Phys, 2006, 39: 2709–2720
19 Wasik G, Gawlik W, Zachorowski J, et al. Laser frequency stabilization by Doppler-free magnetic dichroism. Appl Phys B, 2002, 75: 613–619
20 Siddons P, Bell N C, Cai Y F, et al. A gigahertz-bandwidth atomic probe based on the slow-light Faraday effect. Nat Photon, 2009, 3: 225–229
21 Zhu Y, Gauthier D J, Morin S E, et al. Vacuum Rabi splitting as a feature of linear-dispersion theory: Analysis and experimental observations. Phys Rev Lett, 1990, 64: 2499–2502
22 Notcutt M, Ma L S, Ye J, et al. Simple and compact 1-Hz laser system via an improved mounting configuration of a reference cavity. Opt Lett, 2005, 30: 1815–1817